RESEARCH REPORT

# SOME EXPLORATORY PHOTOELASTIC STUDIES IN STRESS WAVE PROPAGATION



by
M. L. Williams
M. E. Jessey
R. R. Parmerter



Guggenheim Aeronautical Laboratory
California Institute of Technology
Pasadena, California



October 1958

N123-60530S-3825a: T.O. 1
Galcit 90

# SOME EXPLORATORY PHOTOELASTIC STUDIES IN STRESS WAVE PROPAGATION

by

M. L. Williams
M. E. Jessey
R. R. Parmerter

October 1958

This research was supported by the United States Bureau of Ordnance, through the Naval Ordnance Test Station, China Lake, California, Dr. John Pearson, Project Engineer.

Guggenheim Aeronautical Laboratory

California Institute of Technology

Pasadena, California

# SOME EXPLORATORY PHOTOELASTIC STUDIES IN STRESS WAVE PROPAGATION

M. L. Williams*
M. E. Jessey
R. R. Parmerter

## SUMMARY

During the last three years the Guggenheim Aeronautical Laboratory of the California Institute of Technology (GALCIT) has been conducting a photoelastic study of stress wave propagation in solids using a high speed framing camera.

This paper presents a technical description of the camera, now operating at 100, 000 35 mm frames per second at one tenth microsecond exposure time for an elapsed time of approximately two milliseconds. The design capability is expected to approach a half million frames per second. This equipment has been used to record dynamic photoelastic stress fringe patterns in various specimens under impact loadings. Typical experimental records of wave propagation in cracked plates, layered media, compressed bars and beams, and cross sections of rocket heads are included in this report.

## I. GENERAL DESCRIPTION

In 1955, Sutton[1] as part of his doctorate thesis at the California Institute of Technology presented a series of dynamic photoelastic fringe patterns in a rectangular plate under impact compression. To record the data he made use of a high speed framing camera developed at the Institute by Ellis[2] for cavitation studies.

The unique feature used in this equipment was a repeatedly pulsed Kerr cell which operates as a shutter based upon an electrical rather than a mechanical time base. The principle of operation is essentially that if two parallel plates immersed in a closed container of nitrobenzene are charged, the fluid becomes optically birefringent until the charge is removed.

*M. L. Williams, Associate Professor; M. E. Jessey, Research Engineer: R. R. Parmerter, Graduate Student, California Institute of Technology.

Having a fast shutter thus solves the first problem. Next one desires stationary film upon which to record the events, thus obviating the necessity for introducing mechanical motion. The Ellis design used a circular drum whose longitudinal axis coincided with the optical axis and was collinear with a shaft driven at high speed by an air turbine. The end of the shaft was tent-beveled with two 45 degree plane cuts, one of which was blackened and the other polished to a mirror finish. The image coming along the optical axis through the Kerr cell was thus turned at right angles by the mirror and flashed to the stationary film track. The shuttering of the cell coupled with the rotation of the mirror printed successive events on the film strip.

Whereas some experimenters have used multiple light flashes, Ellis achieved satisfactory results using a two millisecond continuous flashtube light source which operated from the discharge of a bank of capacitors.

The last essential ingredient of the first design was a mechanism to synchronize the timing in order that the light was on and the camera recording while the desired event was occurring. Ellis solved this problem by combining a time delay and duration timer.

Upon observing Sutton's results which were not directed toward studies of stress wave propagation per se, it appeared that the experimental set up could be adapted to investigate stress waves in various geometries of engineering interest as a primary objective. Accordingly a second camera assembly has been built incorporating several state of the art improvements and modifications on the basis of experimental convenience and solely dynamic photoelastic objectives.

The main features were (1) reasonably high framing rates, of the order of a half million frames per second, (2) relatively larger optical field to study larger models, (3) long enough time history of the events to permit studies of wave reflection and refraction phenomena in models with low characteristic velocities, (4) a precise start-stop and timing control, and (5) a reliable, safe, and simply operated design.

The preceding requirements necessitated some changes to the basic design. For example, the larger field introduced problems of light

intensity, already critical because it is necessary to have a very high film speed or emulsion sensitivity if it is to be activated in exposure times of 50-100 millimicroseconds. A ten inch diameter field has been attained by using larger collector lens, opening the gap on the Kerr cell plates at the expense of increasing the operating voltage to 20, 000 volts, using only one 45 degree planar mirror cut on the turbine shaft - thus requiring more careful dynamic balance detail design, and increasing the diameter of the film drum. While 35 mm pictures are presently being recorded at 100, 000 frames per second, the turbine is being run at less than half the rated speed and hence 200, 000 frames per second seems assured. At the expense of reducing the image size to 16 mm, provisions have been made for printing twice as many pictures, at the same exposure time, thus again effectively doubling the framing rate. These last two items have not been demonstrated in practice however as it has been the experimental philosophy to increase the turbine speed slowly - and as required for the specimens under consideration - so as not to come upon a critical vibration speed unexpectedly.

A magnetic pickup senses the passage of a 128 toothed gear mounted on the turbine shaft. Each passage generates a pulse which is amplified and formed into a rectangular shape which activates the Kerr cell. Exactly 128 pulses are guaranteed by passing the pulses through a counter containing a gate circuit which closes after the 128 pulses have passed. Overprinting on the film track is thus prevented.

In over fifty runs on the equipment, there have been two failures to operate, one due to a burnt out flash tube and one due to a faulty trigger circuit on the load application mechanism for the model.

## II. DETAIL DESCRIPTION

The camera design was broken down into eight major components as indicated on the block diagram (Figure 1) by appropriate dash numbers:

- 1 Camera Assembly
- 2 Kerr Cell
- 3 Photoelastic Bench
- 4 Control Chassis

- 5 Pulse Power Amplifier
- 6 Light Source
- 7 Initiator Circuit
- 8 Input Power Control Unit

A isometric drawing of the physical layout is shown in Figure 2.

- 1: Camera Assembly. A schematic drawing of the assembly is shown in Figure 3. Its main function is to provide a light tight housing for the pulsed images which have passed through the Kerr cell. After the images are focused through appropriate lens (Bausch and Lomb, Baltar, 100 mm, f/2.3) they are reflected through ninety degrees by the rotating mirror and onto the stationary film track. In Figure 3, most of the necessary items are shown including the general design of the mirror itself. Whereas in the earlier Ellis design V-wedge mirror planes were used, one single plane at forty-five degrees to the turbine axis was employed. In this manner more light was gathered but the turbine shaft was unbalanced. A fish-mouthed sleeve with a circular hole for light passage was therefore designed in order to provide the necessary dynamic balance. A critical speed calculation, assuming clamped bearings, carried out in the Analysis Laboratory using the analog computer indicated that the first or lowest critical bending frequency would be at approximately 120, 000 rpm.

Located behind the mirror assembly is the timing wheel. As each of its 128 teeth pass the magnetic pickup - the miniature model produced by Electro Product Laboratories - a voltage signal is generated. A typical signal record is shown on the oscilloscope record (Figure 4a). While it may be remarked that the record has marked deviation in peak outputs as well as a general overall oscillatory character, the control chassis will accept and easily distinguish voltage signals from 10 millivolts to 10 volts. Such four decade sensitivity has proven more than adequate.

The images reflected from the mirror fall upon the film track, wherein the film lies stationary during a run. The Tri-X or Ilford 35 mm high sensitivity film with a rated speed of 200-400 ASA is stored in 100 foot rolls in a manually, or optionally a motor driven, operated

Mitchell camera magazine. The sprocket assembly from a Cunningham Combat Camera was modified to feed the film into the film track. After some experimentation it was found satisfactory to push the film through. Considering that there was nearly 10 feet to feed, the success of this operation seemed to hinge upon holding the film track dimensions and not permitting local buckling of the strip. After the initial 10 feet was loaded, the cranks on the Mitchell film holder of course permitted the remainder of the roll to be pulled through without difficulty.

As will be observed on Figure 3, a prism was installed on the front plate to permit focusing the image. The dimensions are adjustable on the adapter so that the light path to the film track and to the frosted glass on the adapter were the same. It was also found convenient to design the adapter to accomodate a 35 mm single frame Leica camera to record trial runs to check light intensity without exposing, and developing, a complete 10 foot film strip.

As shown in the photograph (Figure 5) the entire camera assembly was rigidly constructed of metal, except the front plate which was made of plywood to minimize the weight, and was mounted on three adjustable legs to provide levelling and height adjustment.

– 2: Kerr Cell. This component (Figure 6) was fabricated in the Chemistry Department and operated as designed. It is not a new development[3] and its principle of operation is described in most text-books in physics. Certain substances become birefringent when they are placed in an electric field. This is the well known "Kerr effect". The birefringence is proportional to the strength of the electric field, and thus, for a given geometry, to the applied voltage. By appropriate choice of voltage, the cell can be made to act as a half-wave plate, and will rotate the plane of polarization of the light through $90^{\circ}$, provided the plane of polarization of the incident light is $45^{\circ}$ to the principle optical axis of the cell.

The light from the photoelastic set up is therefore polarized at $45^{\circ}$ to the principle axis of the Kerr cell. It passes through the cell and is blocked by a polaroid which is oriented at $90^{\circ}$ to the plane of polarization of the light (In Figure 7, the top of this polaroid is just

visible behind the mounting block). However, when the Kerr cell is pulsed, the light is rotated $90^{o}$ in the cell, and is able to pass through this polaroid.

The device thus acts as a shutter, with a speed which is determined by the length of the applied pulse and the relaxation time of the nitrobenzene. As the relaxation time is many orders of magnitude less than the currently used $10^{-7}$ second pulse, it has no effect in our case. At the other extreme, if the cell is open too long - many orders more than in this design - a lower limit of operation is reached at which the nitrobenzene boils due to the applied voltage and causes optical distortion of the transmitted image.

The 128 signals per revolution which are sensed by the magnetic pickup from the timing disk, are chopped, formed, amplified, and ultimately applied to the Kerr cell. Thus the time between the one tenth microsecond pulses is determined by the turbine speed alone, and is always in precise syncronization with the rotating image so that uniformly spaced frames, without overlap, are obtained.

Besides polarizing the light when the voltage is imposed, the cell has the additional feature of filtering the white light source to the extent of giving nearly monochromatic light without the necessity of introducing additional filters which would of course reduce the already marginal light intensity.

It might also be mentioned that while the liquid is sealed within the cell, nitrobenzene is somewhat toxic and consequently the experiments are conducted in a ventilated room.

– 3: Photoelastic Bench. The optical system (Figure 9) is standard and self-explanatory except that the lens used are not believed optimum for the set up. They are mainly GALCIT equipment from stock and it is anticipated that improvements can be made by designing new items for this application. The present system has, however, operated satisfactorily, and the question is merely one of potential improvement.

When the light source is fired, it remains lit for approximately two milliseconds, the middle portion of which is essentially flat. The light is collected by a 10 inch lens and a non-parallel beam passes through

the model area. Quarter plates are used to give circularly polarized light. The converging beam is passed through another lens and quarter plate and thence into the Kerr cell, through the Kerr cell polarizer, and into the camera.

Through the tests to date there has been no noticeable distortion of the image due to using converging light either through the model or the Kerr cell.

In most of the tests conducted so far the drop rig, shown in Figure 9, was employed. While other loading devices are deemed more appropriate in further experimentation, the drop rig was the simplest with which to carry out the initial tests. A steel ball was restrained by a magnetically operated plunger at the top of a vertical tube. Upon its release downward to impact upon the specimen, it interrupted a photo-cell circuit which provided the input to an initiator circuit to be described presently. Other loading mechanisms would likewise provide an initial signal to trigger subsequent action.

– 4: Control Chassis. Returning to the magnetic signal picked off the timing disk, it is fed into the control chassis (Figure 1) to be amplified and formed into a rectangular pulse on its way toward the Kerr cell. From the original signal given in Figure 4a the resultant signal shown in Figure 4b is generated. Each pulse rises to an amplitude of 10 volts and returns to zero in one microsecond. The rise time may be observed in the figure. After forming, the pulse, which is monitored by a Berkeley Universal Counter (Model 550 I) for the visual information of the experimenter, is fed into the gate circuit which, when triggered, passes into a seven stage binary strip. The binary count is displayed on the control panel (Figure 10) and runs through 128 counts - the number of teeth on the timing wheel. When the count is complete, the gate circuit closes, the pulses stop and the Kerr cell remains closed thus preventing overprinting inasmuch as the camera dimensions are such to provide 128 35 mm pictures around the periphery*.

*Actually four or five pictures at an indeterminant point during the run are lost due to the cut out for the film magazine and blanketing by the prism.

– 5: Pulse Power Amplifier. Inasmuch as the 10 volt signal from the control chassis is considerably less than that required to open the Kerr cell, it is amplified to approximately 20 kilovolts. With the exception of the 21 kilovolt, 1.5 Mfd capacitors and the Solar regulating transformer, all components were GALCIT designed and represented a significant amount of time devoted to electronics. The amplifier is separately controlled as a safety precaution. Its general layout and size may be observed in Figure 5 or Figure 10 where it lies to the left of the control panel.

These signals then are those which open and close the Kerr cell electrical shutter for the camera.

– 6: Light Source. The light source is another important component inasmuch as a critical problem in high speed photography is a proper matching of light intensity and film speed. Following Ellis' experience, a xenon-filled General Electric Model FT 524 Flash tube rated at 5 kilovolts, 250 Mfd was used. The power supply consisted of a bank of 10 kilovolt, 25 Mfd capacitors; when the design voltage of 5000 was reached, the light, coordinated with the drop rig photocell signal by appropriate time delay units, was fired.

A photograph of the unit (Figure 11) shows the coiled nature of the flashtube geometry which did not give uniform intensity and led to streaks on some of the resulting pictures. At the expense of losing light a frosted glass was inserted between the source and the collector lens in later tests to provide diffused light.

The spectral distribution of intensity for the source is given in Figure 12 and is seen to be relatively flat over the light sensitivity band of the film. The life of the flash tube for this type operation seems to be in the vicinity of 100 firings when operated intermittently at voltage discharges of 5000 volts and below. The light will not fire if the voltage is lower than 2000 volts.

– 7: Initiator Circuit. The photocell circuit (Figure 1) is a standard GALCIT item and has been used successfully for several years. One unusual feature incorporated into the drop rig pick up (Figure 9) is the relatively small light source used. Its focal point is interrupted by the ball to trigger the circuit. In the first tests two pickups four inches

apart were used and the velocity of the one inch diameter 0.15 lb. steel ball at impact was determined to be 155 inches per second.

– 8: Input Power Control Unit. The last major component of the camera is the power routing control. The entire system operates from 120 volt AC, 60 cycle; power is routed to the various individual power supplies, Berkeley counter, and auxiliary equipment by appropriate cables.

Generally speaking, with the exception of the separate safety control on the pulse power amplifier, all controls are centralized in the control panel (Figure 10) which contains the time delay units, light source and initiator triggers, the counter, turbine speed control and lubrication indicator, and auxiliary power. This arrangement has considerably simplified checkout prior to testing as well as permitting direct control during experiments.

## III. PRELIMINARY RESULTS

The camera has been used over the last few months to perform a number of exploratory experiments. The specimens tested have been made from one of the standard photoelastic plastics, CR-39[4]. When this plastic is loaded and viewed in circularly polarized light through a quarter-wave plate and polaroid, light and dark lines or fringes appear. For CR-39 subjected to dynamic loading, a given fringe is a line of constant difference in principal strain[2], which itself is proportional to the maximum shearing strain. In order to determine the complete stress field as a function of time, further measurements and analysis of the data is necessary. Our program however has attempted to obtain qualitative data for a number of problems, the most interesting of which are to be discussed.

A drop rig (Figure 9) was chosen as the simplest method of applying a dynamic load in these tests. A 0.15 lb. steel ball is held at the top of a 41 inch tube by a solenoid. Closing the circuit to the solenoid releases the ball, which falls freely down the tube and strikes the specimen at 155 inches per second. The ball trips a photocell, which is located just above the specimen, and this signal opens the gate circuit to the Kerr cell amplifier after a suitable time delay.

Two fields of view have been used, a 2 1/2 inch diameter field and a 10 inch diameter field. The 2 1/2 inch field provides higher resolution of fringes, while the 10 inch field allows a longer time to observe the fringes without interference from the reflection of the stress wave by the boundary. All pictures included are 35 mm and have been taken at 70, 000 or 100, 000 frames per second.

Fracture

Because of the interest at GALCIT in fracture and stress distributions at the point of a crack, it was of interest to see if the dynamic fringe pattern was similar to the static one, predicted by theoretical analysis[5], as well as to compare it with the data obtained by Wells and Post[6], using individual spark photographs. For this reason a 1.2 x 2.5 inch rectangular specimen 1/4 inch thick was prepared. A small slot 1/4 inch deep and ten thousandth of an inch wide was cut in the top to accommodate a Shick razor blade, chosen for its low aspect ratio and consequent rigidity (Figure 13). The blade protruded approximately 1/16 inch over the top of the specimen and was contacted by the falling steel ball. Figure 13 shows interesting sections of the complete record obtained.

First of all it is observed that as the force introduced by the ball is transmitted to the specimen, the stress gradually builds up without any immediate fracture. Furthermore the gross appearance of the fringe pattern possesses the characteristic "bug-eye" appearance predicted for the static case[5] (Figure 14), spoiled somewhat of course in sharpness because the width of the crack is actually finite, and hence the vertex is rounded. With time the load builds up as indicated by the increasing number of fringes until at about the third or fourth picture (separated timewise by 14.5 $\mu$ seconds) the ultimate load is reached and the crack appears to accelerate. The time of running is affected by many factors of course, not the least of which are the generally compressive nature of the stress field, the local stress condition after machining, and the interference of reflected waves which take approximately 20 microseconds to cross the specimen.

The first clear indication of the propagation may be noted on the ninth frame after contact where the gross "bug-eyes" have given way to an elliptic-like shape. This qualitative characteristic pattern predicted statically (Figure 14) may be associated with an antisymmetric stress field due to the blade not being precisely centered in the slot and hence contributing a high localized shear stress. In the eleventh frame the "bug-eyes" are beautifully reestablished at the crack front and carry very plainly through six frames until the crack breaks through and the stress field unloads completely in the latter frames of the second row.

Returning to the first frame for a moment it will be noted that the ball emerging from the tube is pressing upon the razor blade. Beginning in the third row, where several frames are missing as may be noted by the coded numbers on the film strip, the ball has now pushed the blade into the plastic and has itself contacted the specimen. Due to a slight antisymmetry the dynamic Boussinesq fringes are not perfectly paired, although the second frame is coincidentally remarkably continuous across the crack (as it should be because the fringe value or shear is zero at the crack). These latter frames are included to give a striking visual illustration of the complex interaction to be expected when the waves have time to reflect from free and fixed boundaries.

Before making any semi-quantitative deductions at all from the strips, consider the next specimen, shown in Figure 15. In contrast to the previous case where the crack was loaded, an experiment was tried wherein a similar specimen was inverted and simply supported with the crack on the bottom. It was then impacted on the top as indicated in the figure with the resulting 100, 000 frames per second fringe pattern as shown. (The striations observed, as mentioned earlier, are due to the undiffused helical light source.) Reading from the top left down, the characteristic Boussinesq pattern is exhibited. As it progresses to the supports and across the bar sensing the presence of the crack, a reflected signal observable at strip number 38 and firmly established at 39 indicates the crack progressing toward the load. While the pattern is complex it appears that the crack accelerated too quickly for the quasi-static "bug-eyes" to appear before complete fracture.

In order to explore this point a bit further, a crack front position vs. time plot was prepared based upon reading the film strip in an enlarger and gave the data shown in Figure 16. It is immediately noticed that for this geometry, the loaded crack reached a maximum speed only half that of the unloaded crack. It is interesting to observe the very rapid acceleration in the latter case and the quantitative value of the propagation - 17, 700 inches per second. If one uses Clark's value[4] of the sound velocity, viz. 60, 000 inches per second, the propagation speed can not be less than 30 per cent of the sound velocity, or approximately 50 per cent of the shear velocity.

Considering the qualitative nature of this experiment, the values are in reasonably close agreement with Wells and Post's, although the records seem to indicate that the acceleration - for the unloaded crack - was a bit more rapid than their case which would tend a bit more toward their theoretical expectations.

Layered Media

Another set of experiments pertained to layered media. Such geometries are of fairly wide concern in aeronautics, civil engineering and atomic warfare. Generally theoretical treatment is difficult if not impractical, but the initial tests indicated that two-dimensional tests at least could be conducted simply with quantitative interpretation. In Figure 17, the same drop rig has been used to apply a load to a rectangular specimen of CR-39 which was separated into two pieces separated by a section of electrical tape having of course a different modulus. It was desired to examine the feasibility of recording wave transmission phenomenon such as is illustrated in the figure. To add a bit of additional practical interest, a circular hole was cut in the lower piece of CR-39 and consequently the results show not only a transmission delay but also the passage of the transmitted wave around the inclusion giving rise to a dynamic stress concentration factor. The stress pattern is quite symmetrical with the expected clover-leaf pattern very apparent. Inspection of the film strip in an enlarger indicates that quantitative analysis is perfectly feasible. Hence the effect of parametric changes in materials, relative thicknesses and changes in the shape of the inclusion can be evaluated without undue difficulty.

Simulated Head Studies

The third set of tests to be described relates to the impact of ogive type specimens with variable head angles. Figure 18 shows a set of data using the drop rig and a 70, 000 framing rate which was among the earliest records obtained. Here a qualitative idea of the cone angle magnitude was desired for which the wave front remained essentially planar. In the limit for very small included angles or wedges, one would normally treat the problem theoretically as a one-dimensional wave by simply replacing $r\, d\theta$ by $y$*.

From the records it appears the one-dimensional assumption becomes increasingly accurate for included wedge angles less than 60 degrees.

Following up the wedge tests, another series was run at 70, 000 frames per second for a 90 degree included angle with a rectangular "afterbody" (Figure 19) which was used to compare with the same geometry except it was notched symmetrically (Figure 20). The constricting effect of the notch is quite evident by simply comparing the fringe density in the upper and lower sections. While data interpretation in the vicinity of the corners would be difficult more generous fillets in this region would permit straightforward quantitative analysis inasmuch as the fringe patterns are satisfactorily distinct.

For the final test in this set, the previous specimen was again used except the central part was removed to simulate the cross section of a rocket head (Figure 21), although it hardly need be remarked that the wall thickness is relatively oversize. Again the steel ball was dropped on the point of the head and the resulting fringe pattern observed. The separation and diffusion of the load down the two legs of the "tuning-fork" in a most symmetric fashion is easily observed. Moreover the skew wave front indicates the bending or flexural character of the wave transmission which proceeds through the length of the specimen in very close to the 50 microseconds expected. A fracture occurs at about the fifth frame and the propagating crack runs into the reflected stress field from the maximum stress point at the radius of the inside ogive contour. Fracture is complete by the ninth frame and in all the subsequent pictures the two legs are behaving as two independent bodies.

*While it is to be emphasized that the fringes are not necessarily dilitational - actually they are maximum shear strain lines, considerations of symmetry and boundary conditions usually permit proper interpretation without additional data such as the dynamic isoclinics. This point deserves careful consideration for quantitative analysis however.

## IV. CONCLUSIONS

In reviewing the program, it is believed that the exploratory studies have established that the camera design is satisfactory to achieve quantitative dynamic design data for a considerable number of engineering problems.

It is, of course, obvious that there are places where improvements can be made, most particularly in the optical system where it is known that the optimum system has not been used. Furthermore, a more appropriate loading mechanism should be designed to simplify quantitative analysis; also certain state of the art improvements can be introduced in any research tool. In addition, certain advancements will be required in the theoretical area as well as in determining and interpreting material property data, especially if other than CR-39 is contemplated.

Nevertheless it is the opinion of the authors that an important and convenient tool has been demonstrated for dynamic analysis. The proper quantitative exploitation remains.

## ACKNOWLEDGMENT

The authors wish to acknowledge the able assistance of other present and former members of GALCIT who have contributed to this program. In particular the consultations with Prof. E. E. Sechler and the mechanical design work of Mr. A. E. Gaede has been especially helpful.

## V. REFERENCES


1. Sutton, G. W.: Study of the Application of Photoelasticity to the Investigation of Stress Waves. Thesis in Mechanical Engineering, California Institute of Technology, June 1955. See also an abbreviated version, A Photoelastic Study of Strain Waves Caused by Cavitation. Journal of Applied Mechanics, Sept. 1957, vol. 24, no. 3, p 340.

2. Ellis, A. T.: Observations on Cavitation Bubble Collapse, Thesis in Mechanical Engineering, California Institute of Technology, 1953.

3. White, H. J.: The Technique of Kerr Cells, Review of Scientific Instruments, v. 6, 1935, pp 22-26. See also: Kingsbury, Rev. Sci. Instr., v. 1, 1930, p 22. Beams, Rev. Sci. Inst., v. 1, 1930, p 780. Dunnington, Phys. Rev., v. 38, 1931, p 1506.

4. Clark, A. B. J.: Static and Dynamic Calibration of a Photoelastic Material, CR-39, Report 4779, Naval Research Laboratory, June 1956. See also Soc. Exp. Stress Analysis, vol. 14, n. 1, 1957, pp 195-204.

5. Williams, M. L.: The Stress Distribution at the Base of a Stationary Crack, Journal of Applied Mechanics, March 1957.

6. Wells, A. A. and Post, D.: The Dynamic Stress Distribution Surrounding a Running Crack - A Photoelastic Analysis, Report 4935, Naval Research Laboratory, April 1957. See also Soc. Exp. Stress Analysis, vol. 12, n. 1, 1954, pp 99-116.

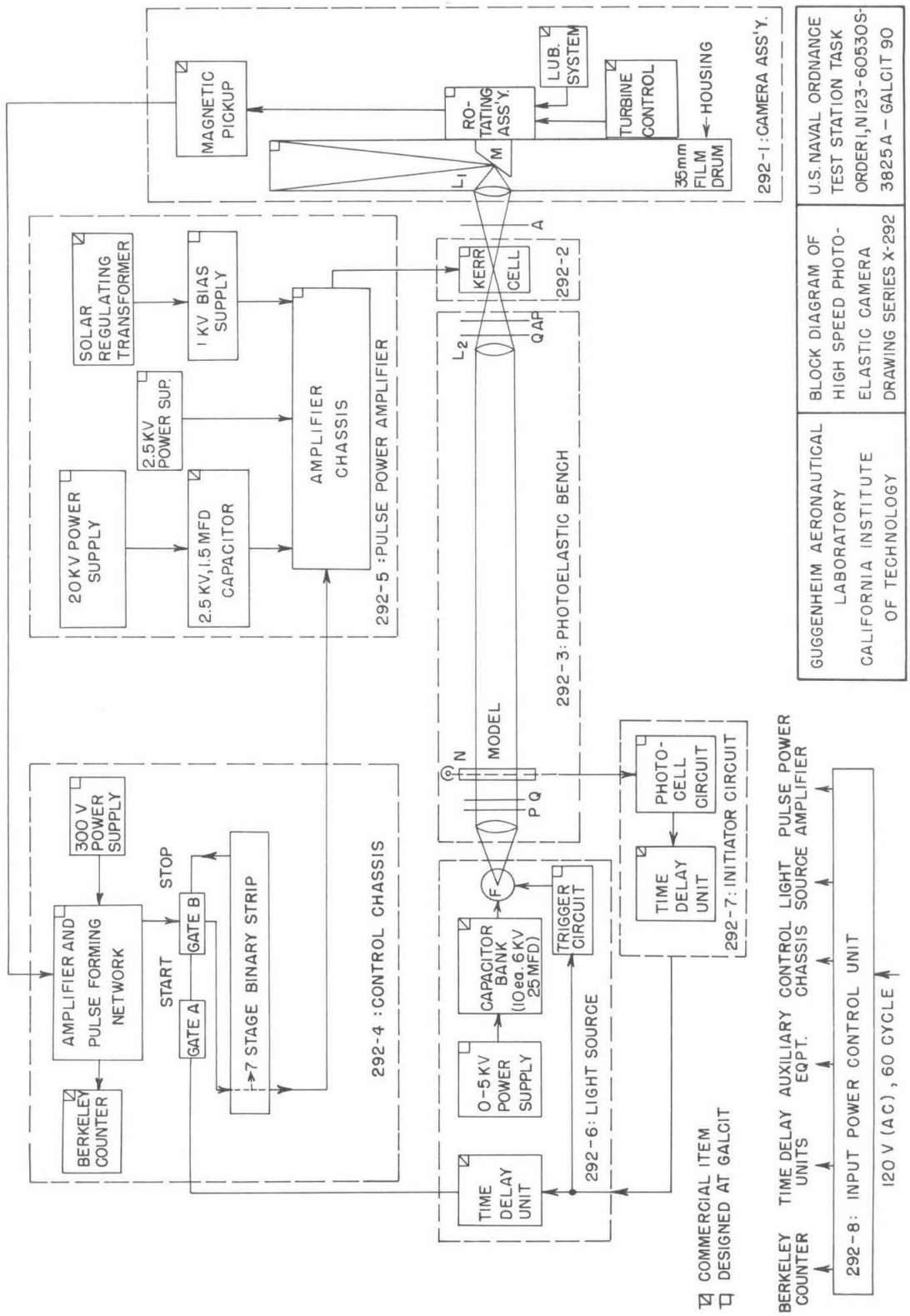


Figure 1. Block Diagram of High Speed Photoelastic Camera Drawing Series X-292.

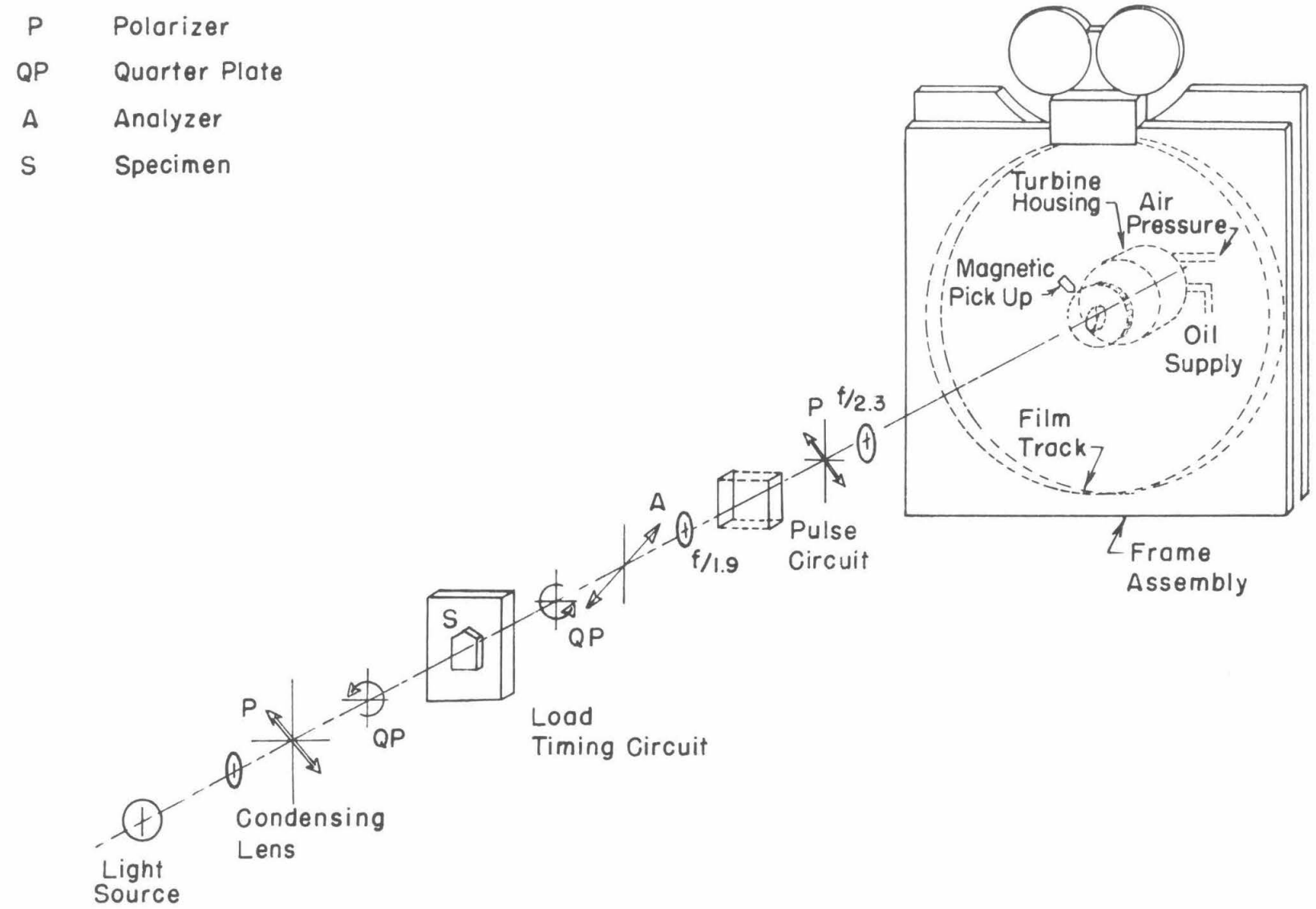


Figure 2. Schematic Layout of the Camera Assembly.

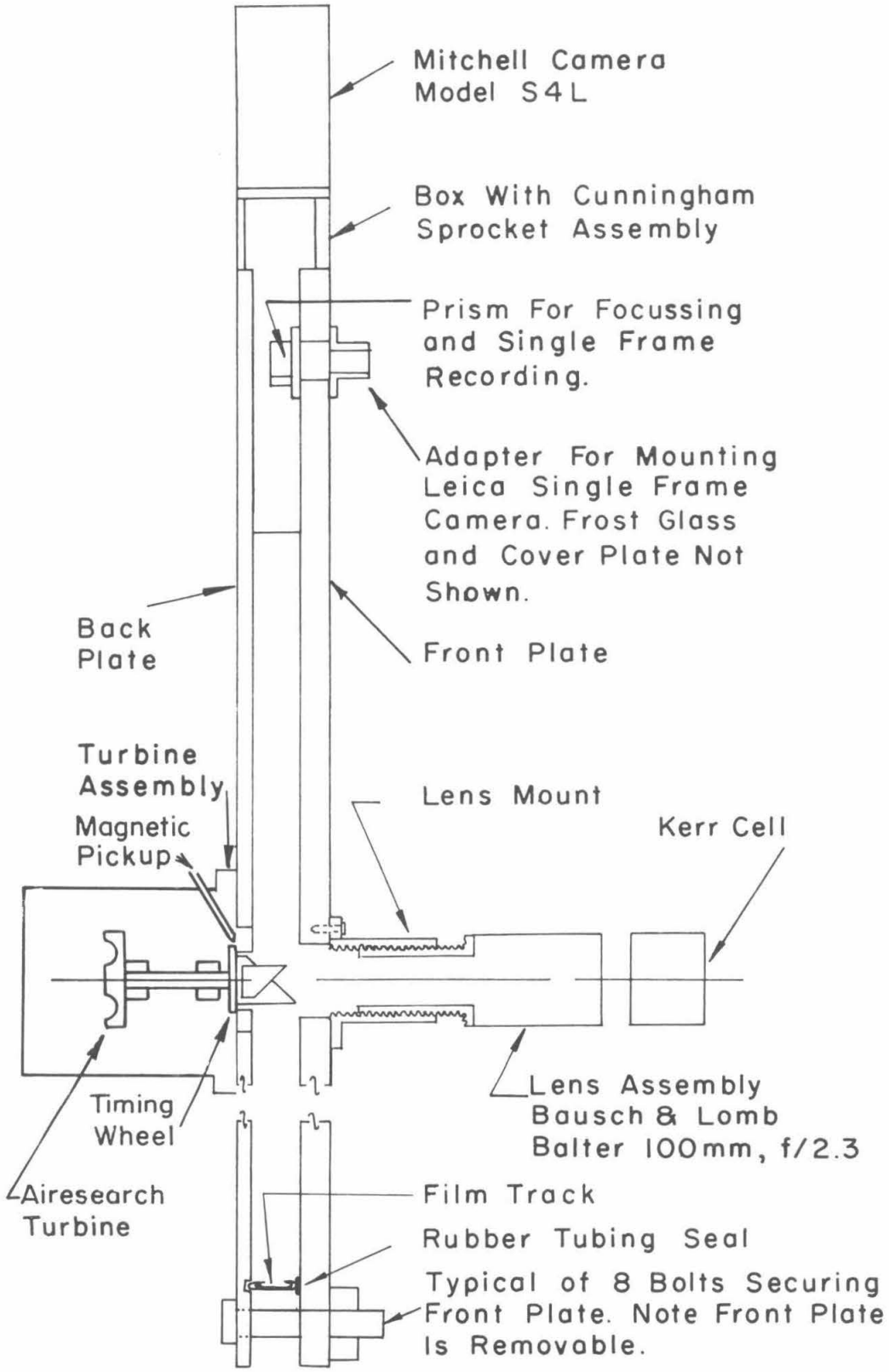


Figure 3. Camera Assembly - Schematic.

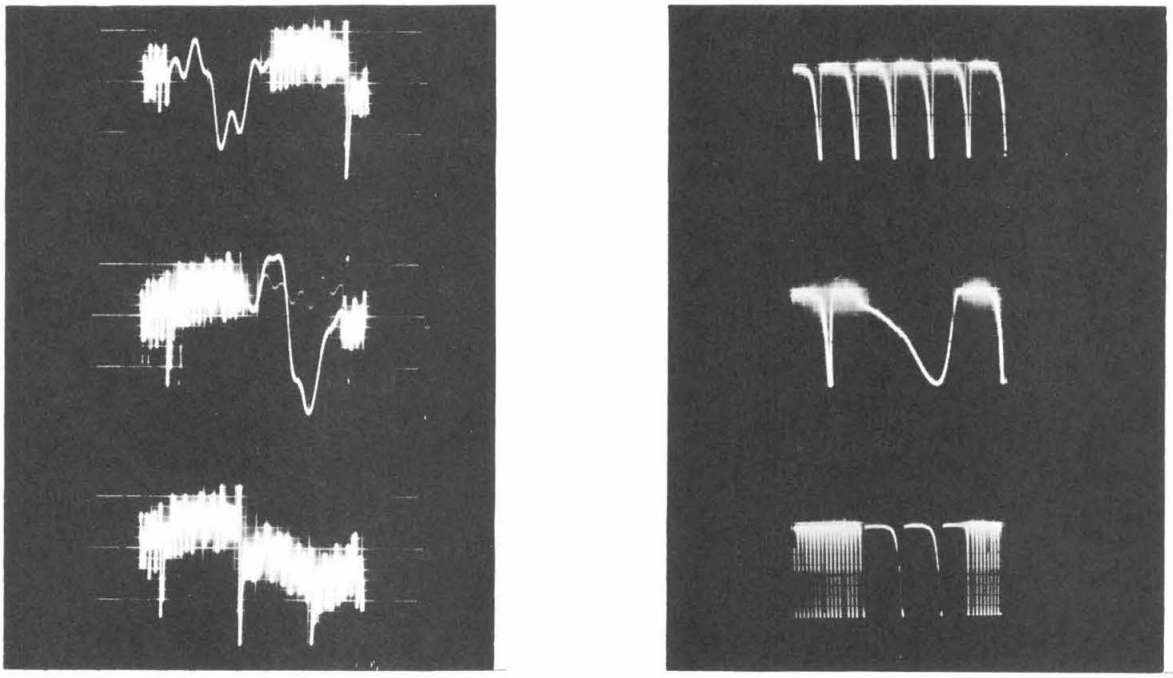

Figure 4.

a. Magnetic Pickup Output.

b. Control Chassis Output.

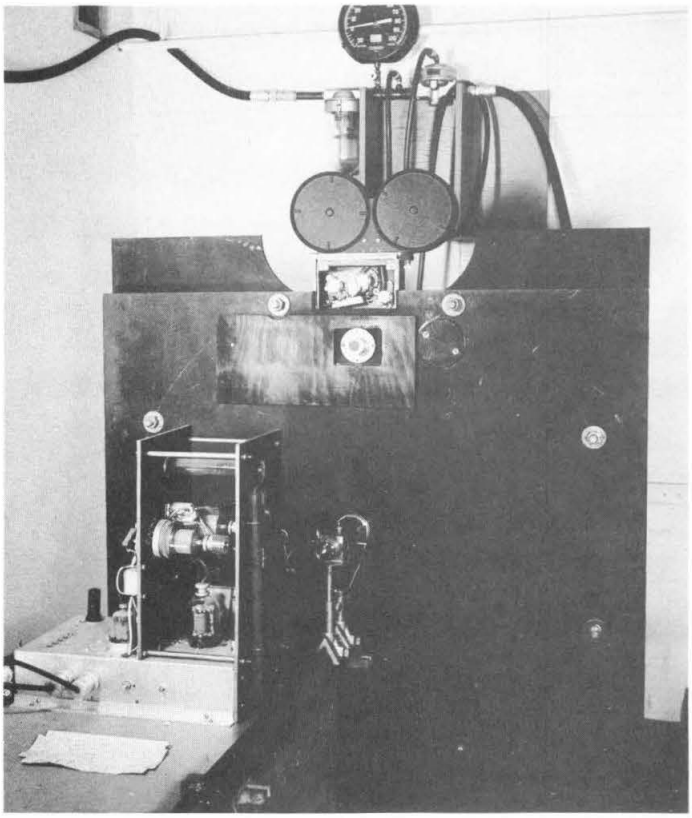

Figure 5. General View of Pulse Power Amplifier, Kerr Cell and Camera.

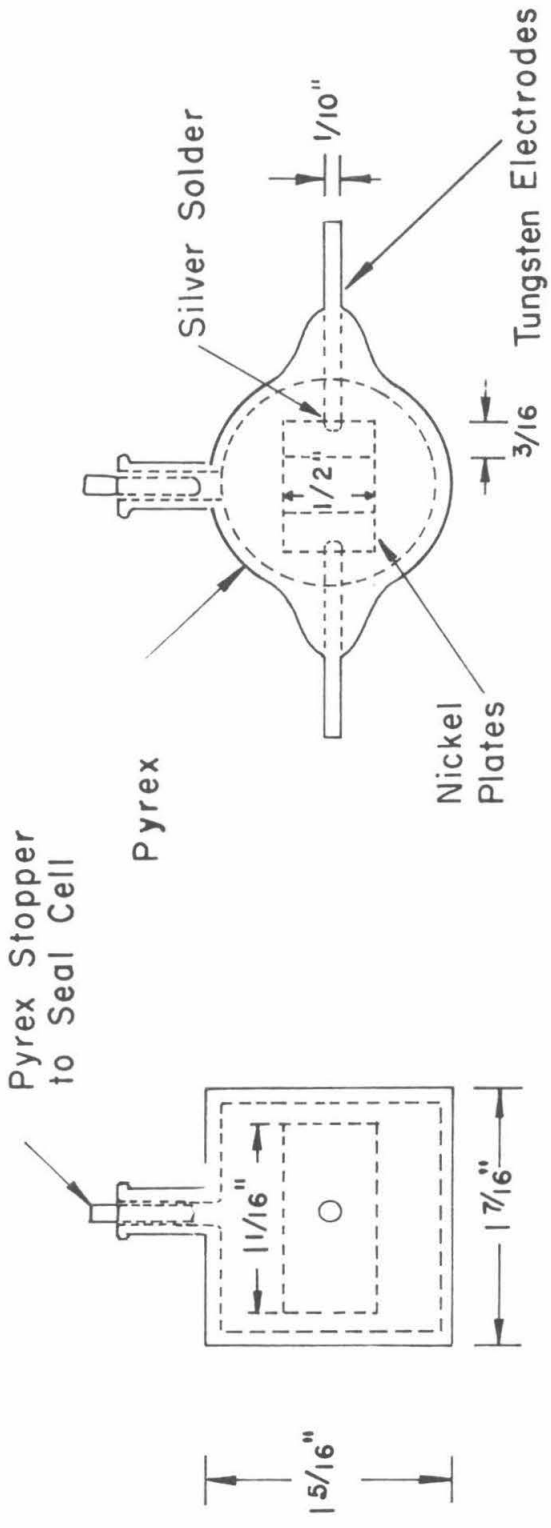


Figure 6. Kerr Cell.

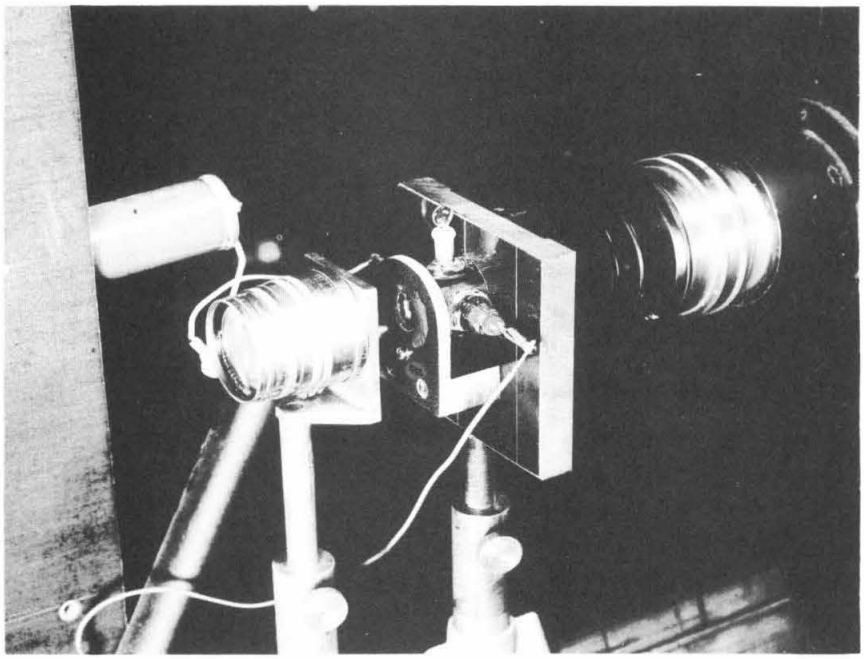

Figure 7. Close up of Kerr Cell.

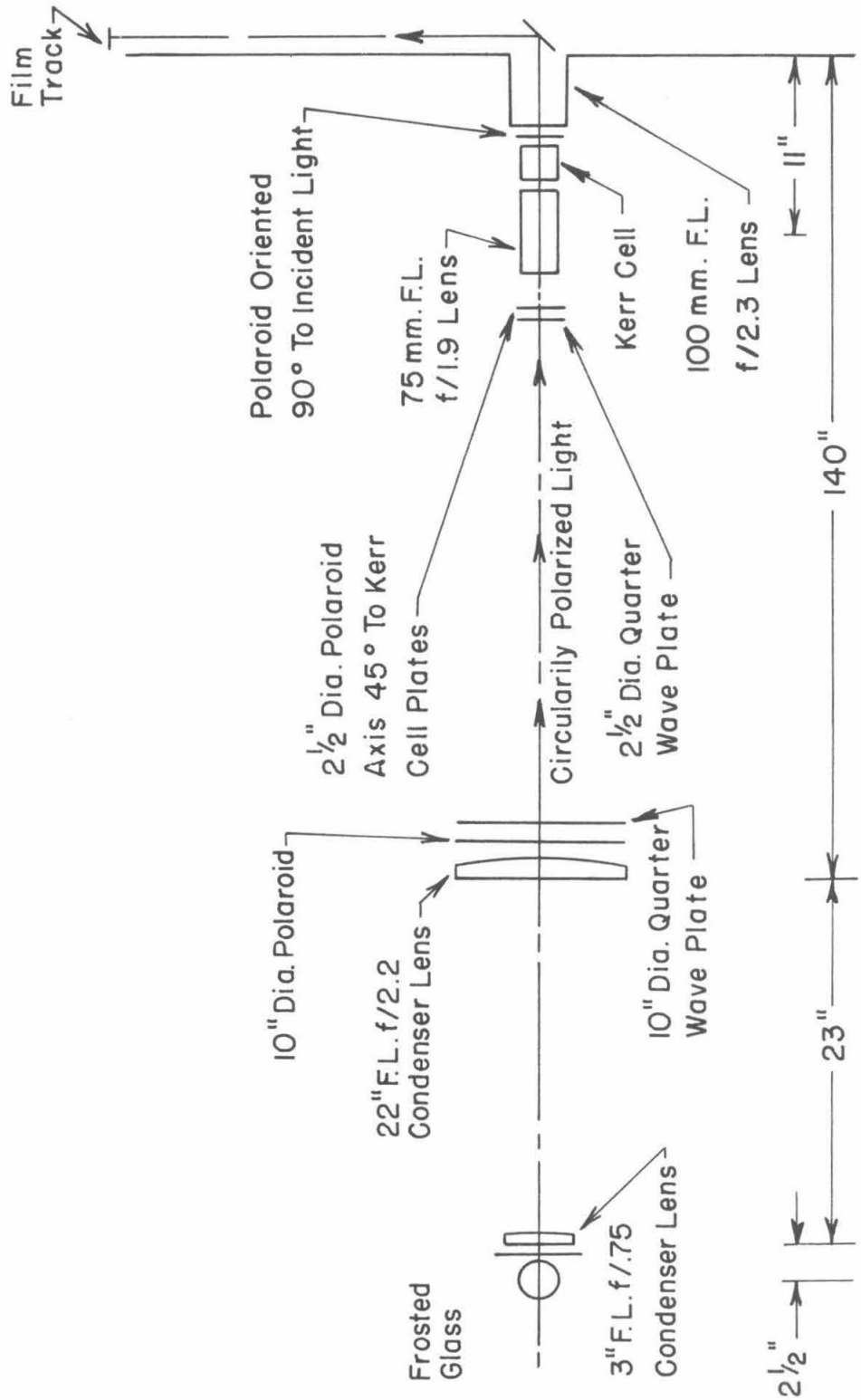


Figure 8. Photoelastic Bench, 10" Field.

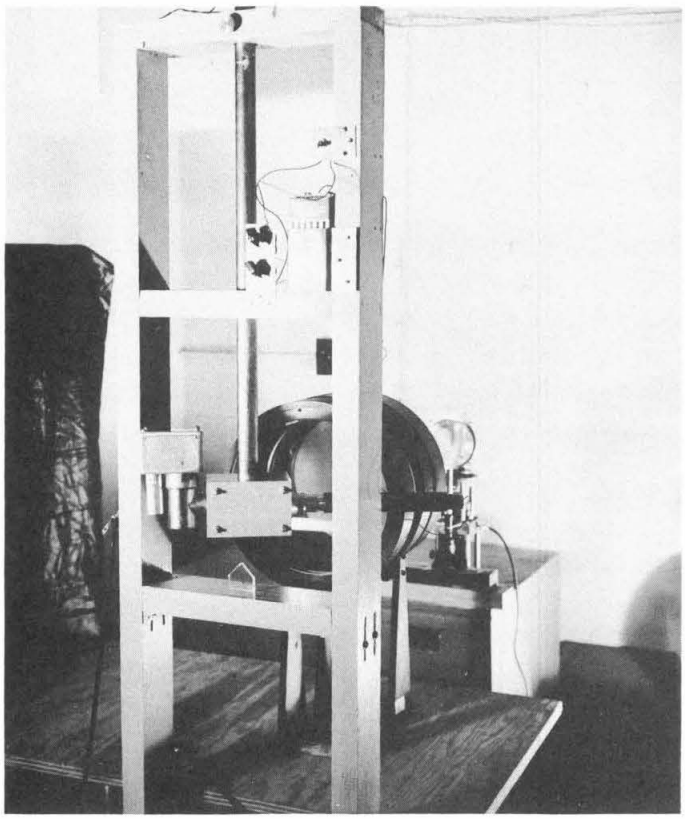

Figure 9. General View at Drop Rig Showing Typical CR-39 Specimen in Place.

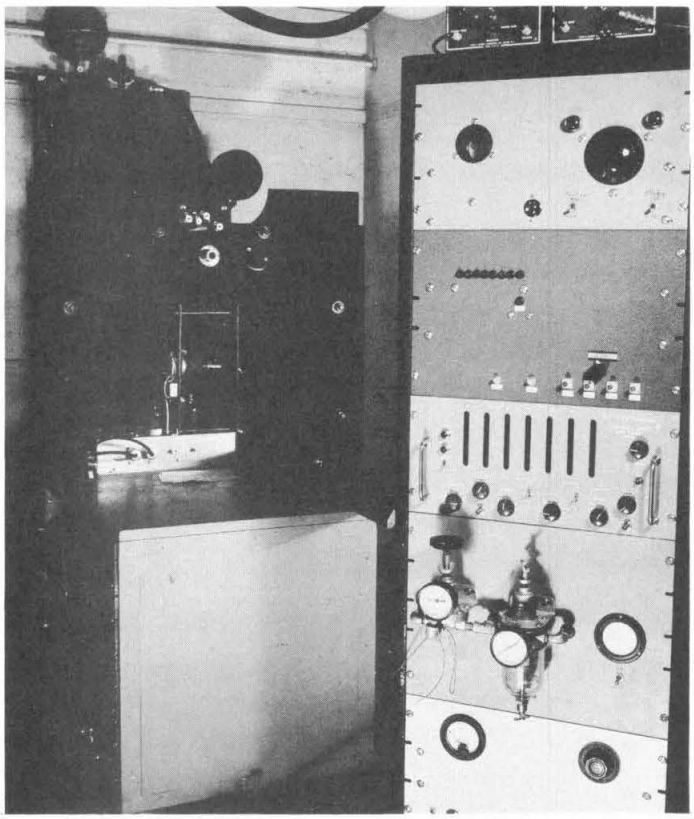

Figure 10. General View of the Camera, Amplifier and Control Panel. From Top to Bottom on the Panel: Two Delay Timers, Light Source Capacitor Control, Firing Panel, Counter, Turbine Control, Photo-cell Control.

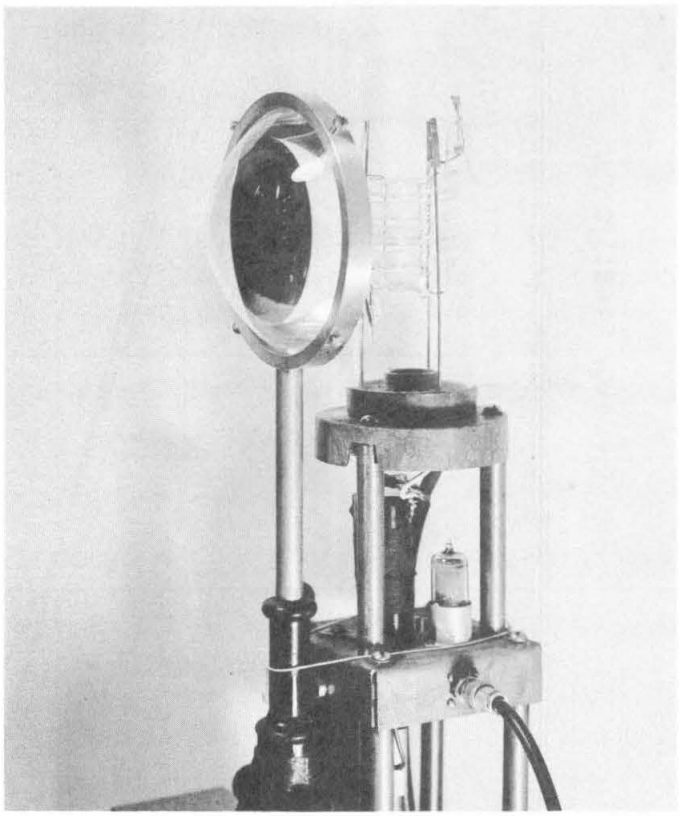

Figure 11. Close up of the Light Source and Collector Lens.

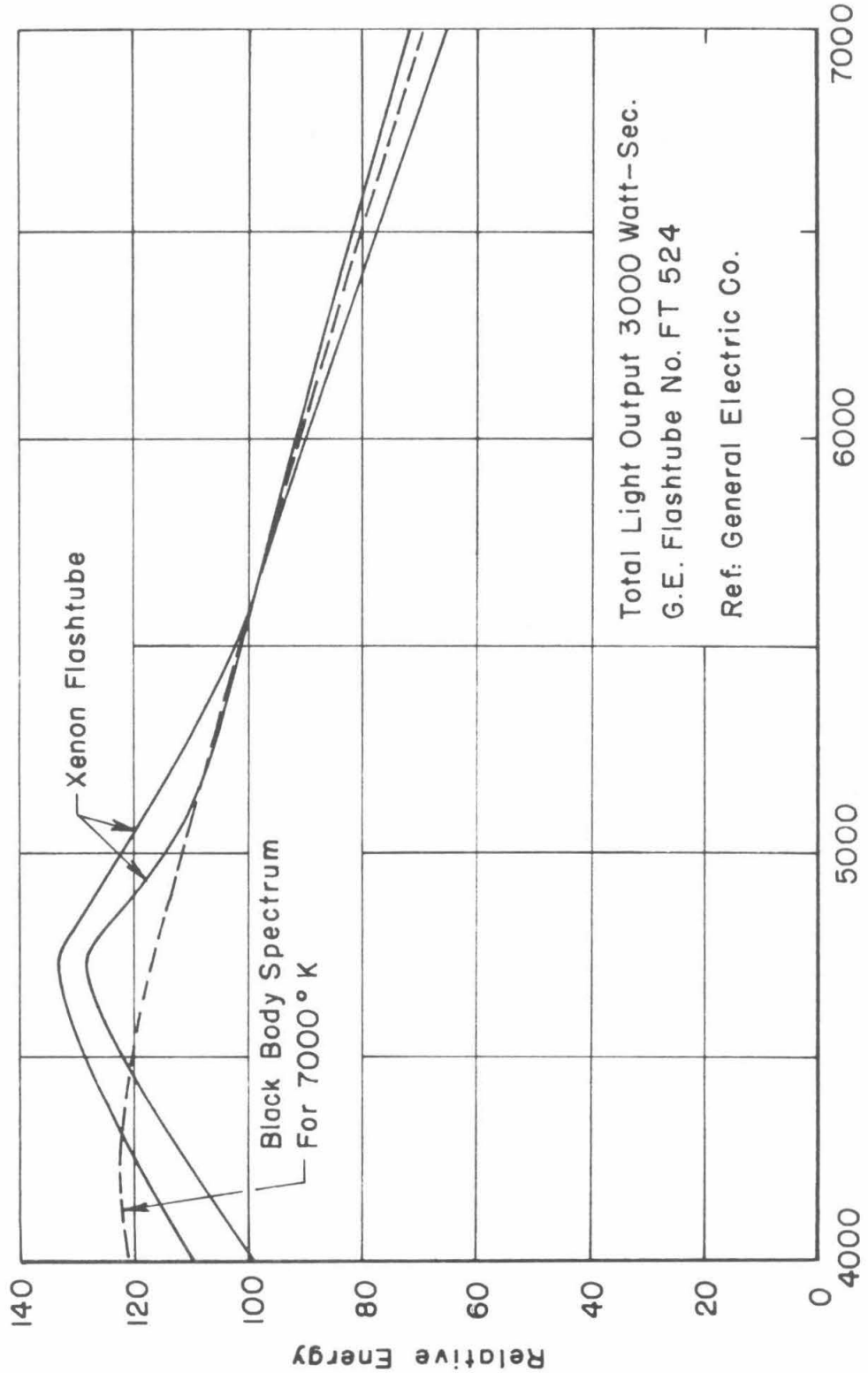


Figure 12. Spectral Distribution for the FT 524 Flash Tube.

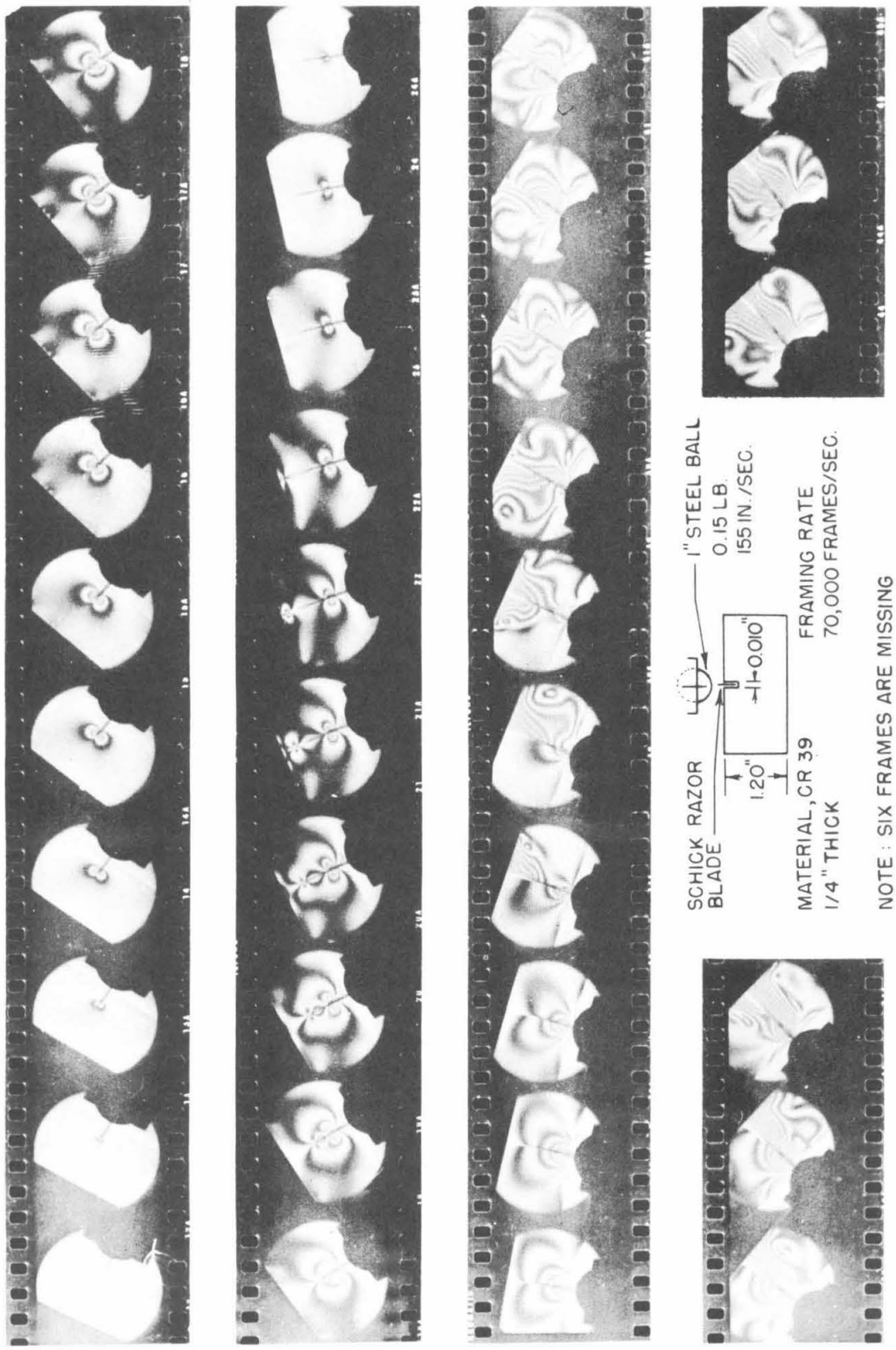


Figure 13. Dynamic Stress Distribution for a Loaded Crack.

Framing Rate 70, 000 Frames per Second.

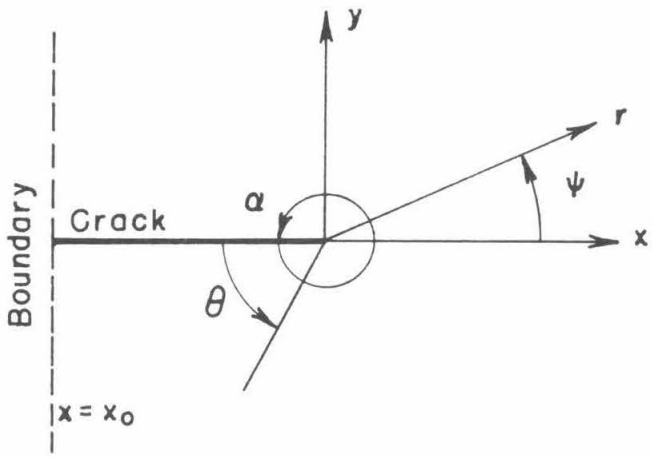


14 a — GEOMETRY

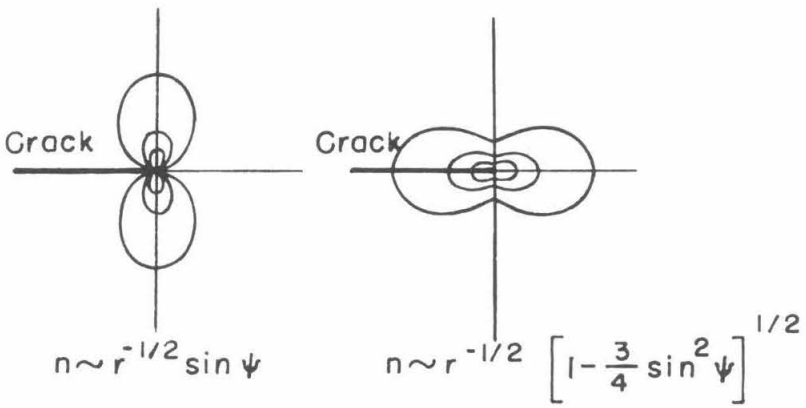


14 b - SYMMETRIC FRINGES

14 c - ANTI - SYMMETRIC FRINGES

Figure 14. Static Isochromatic Fringe Patterns.

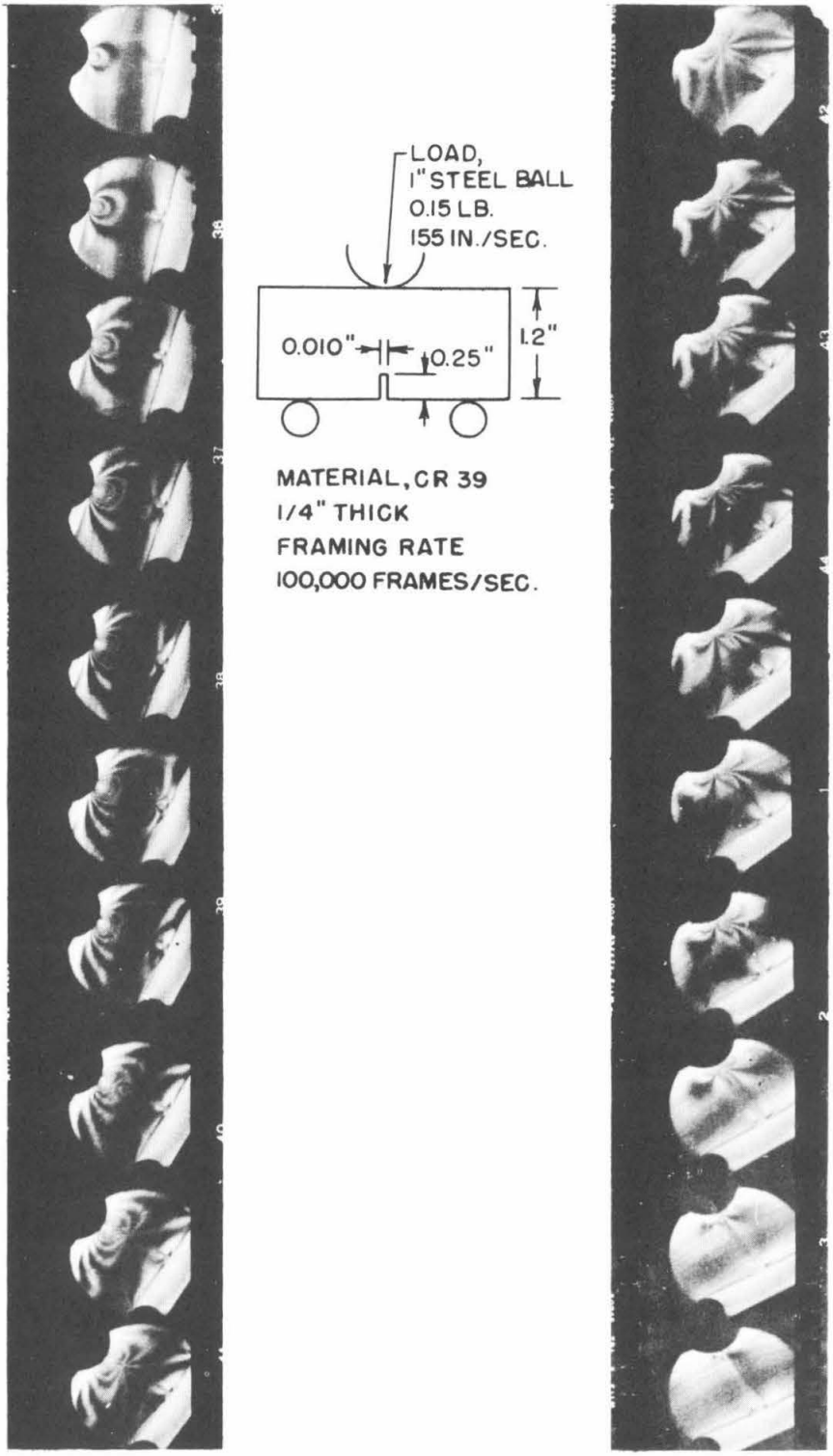


Figure 15. Dynamic Stress Distribution for an Unloaded Crack. Framing Rate 100, 000 Frames per Second

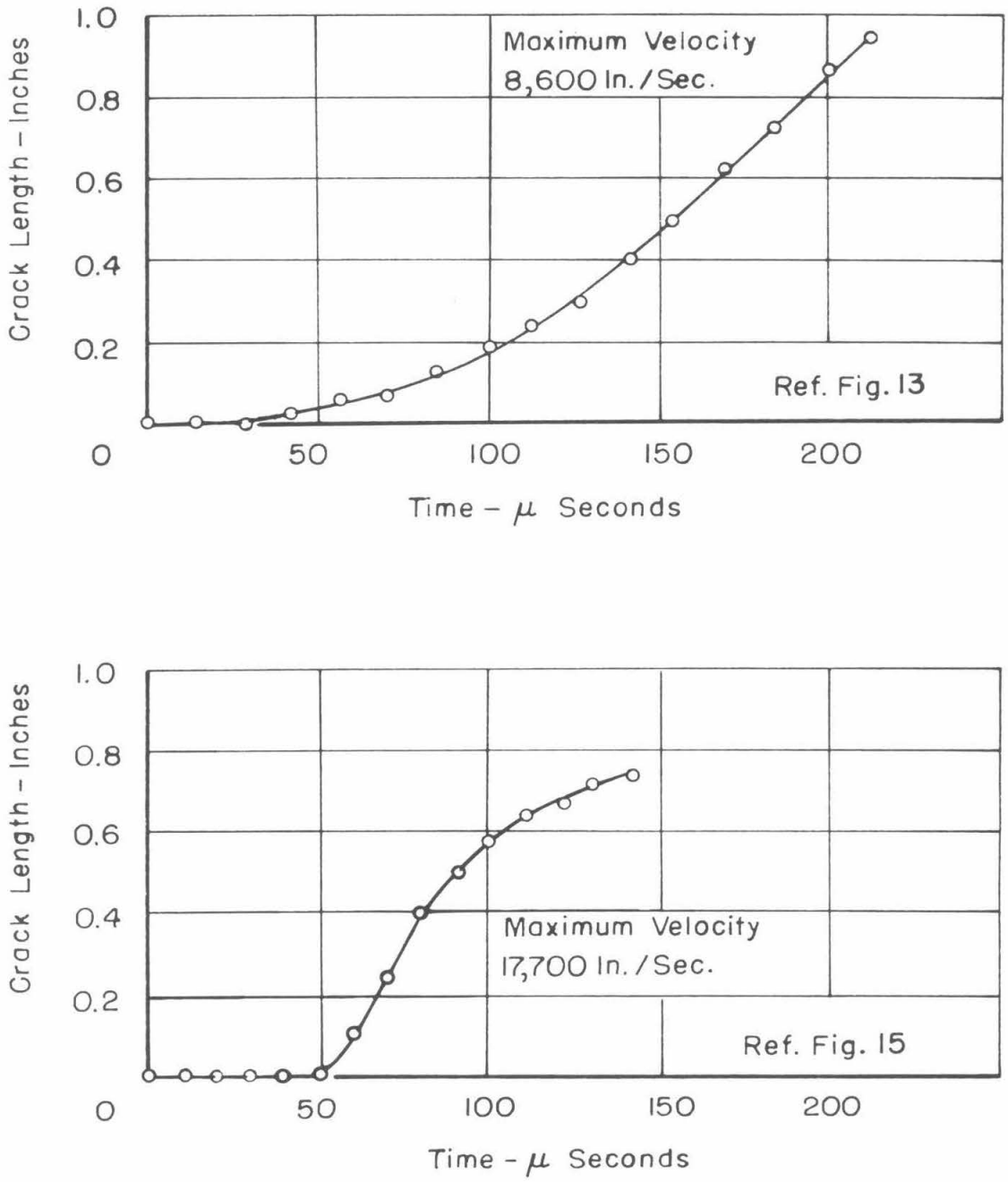


Figure 16. Crack Length vs. Time.

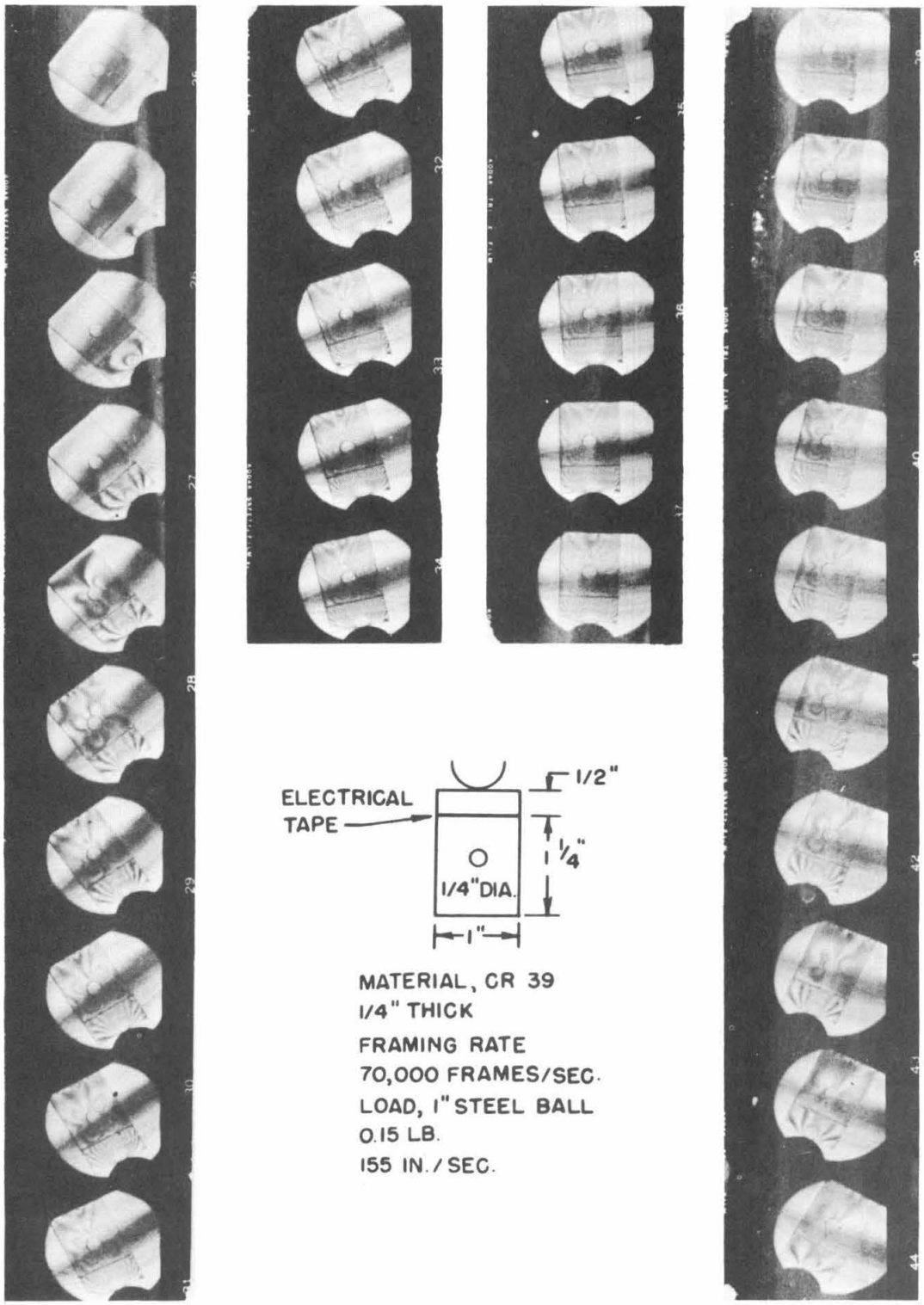


Figure 17. Dynamic Stress Distribution in a Layered Media Having an Inclusion.

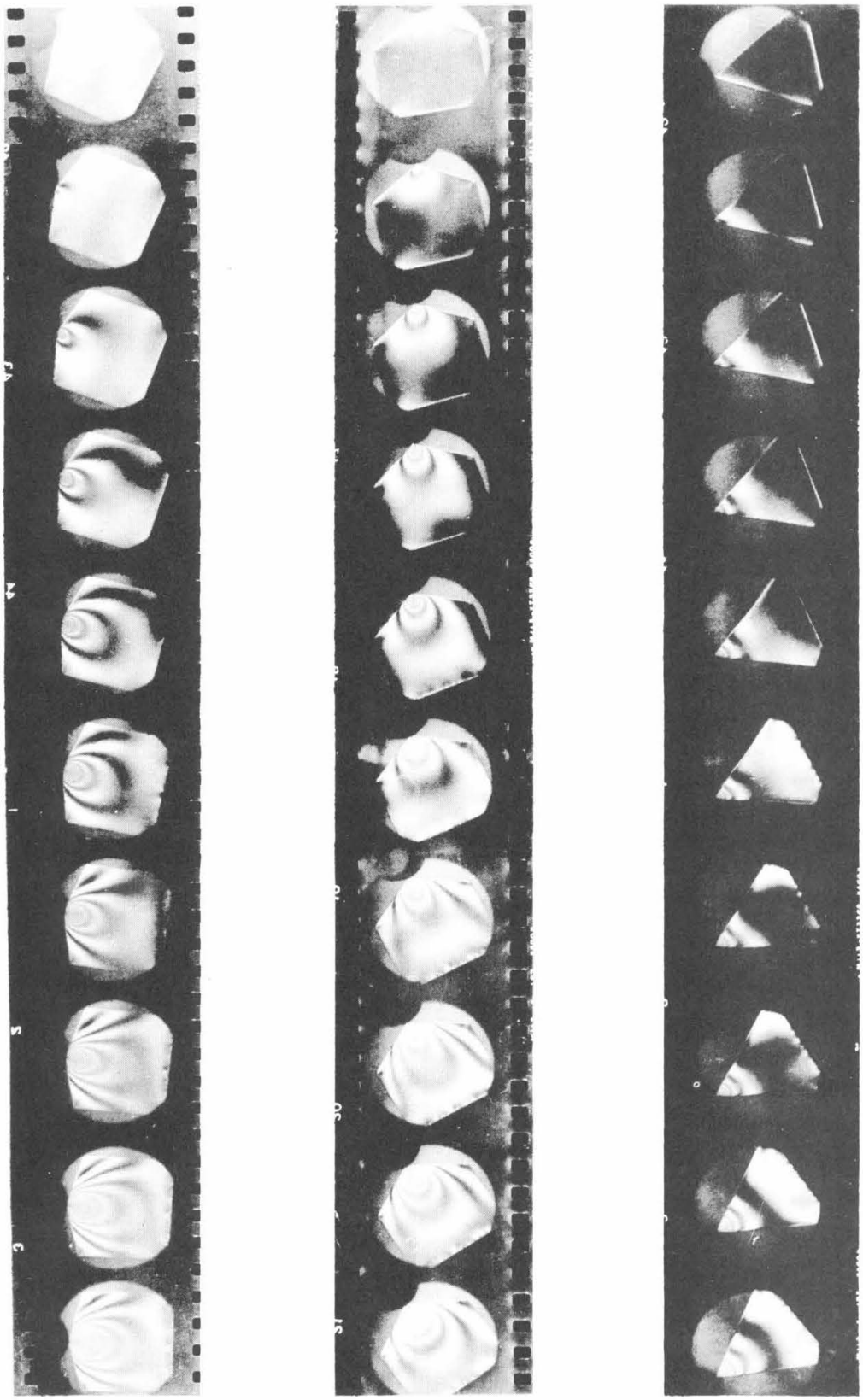

Figure 18. Wedge Angle Effect Under Impact.

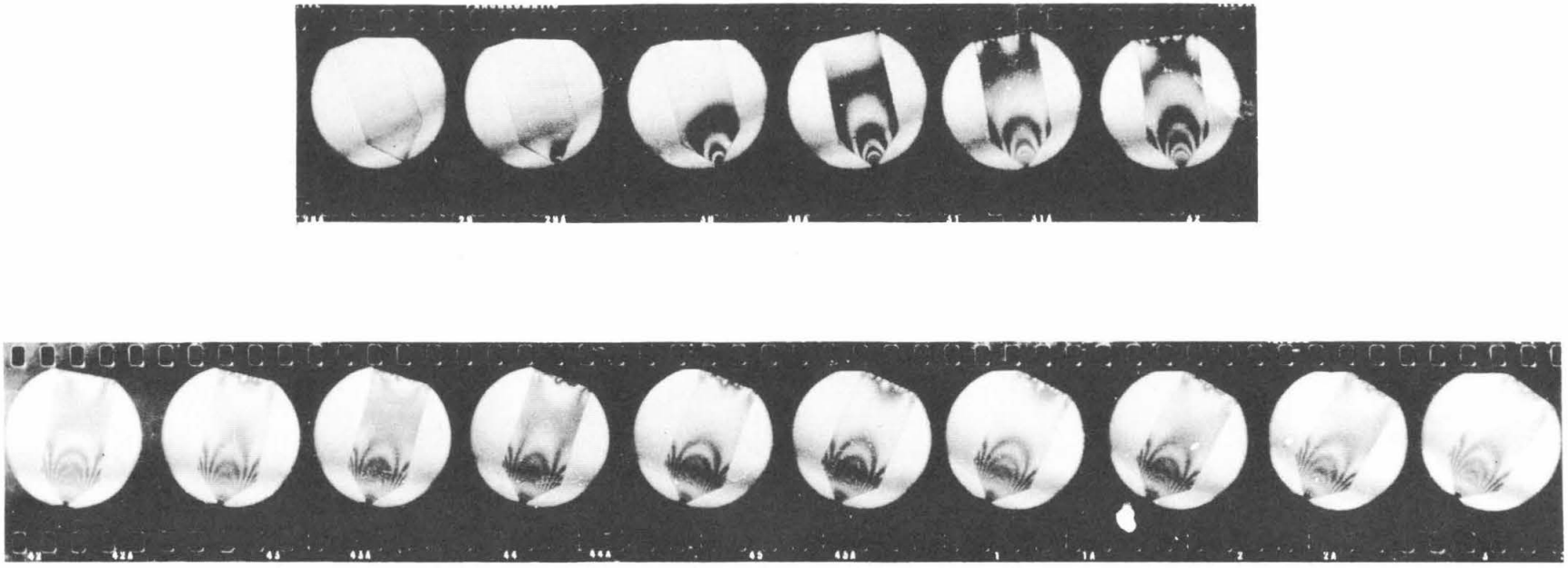

LOAD, 1" STEEL BALL
0.15 LB.
155 IN./ SEC.

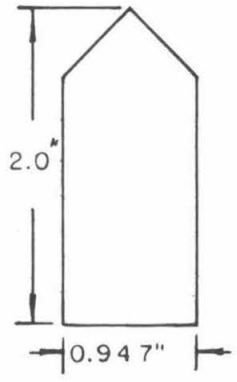


MATERIAL, CR 39
1/4" THICK
70,000 FRAMES/ SECOND

Figure 19. Dynamic Fringe Patterns for a 45° Wedge-Body Configuration.

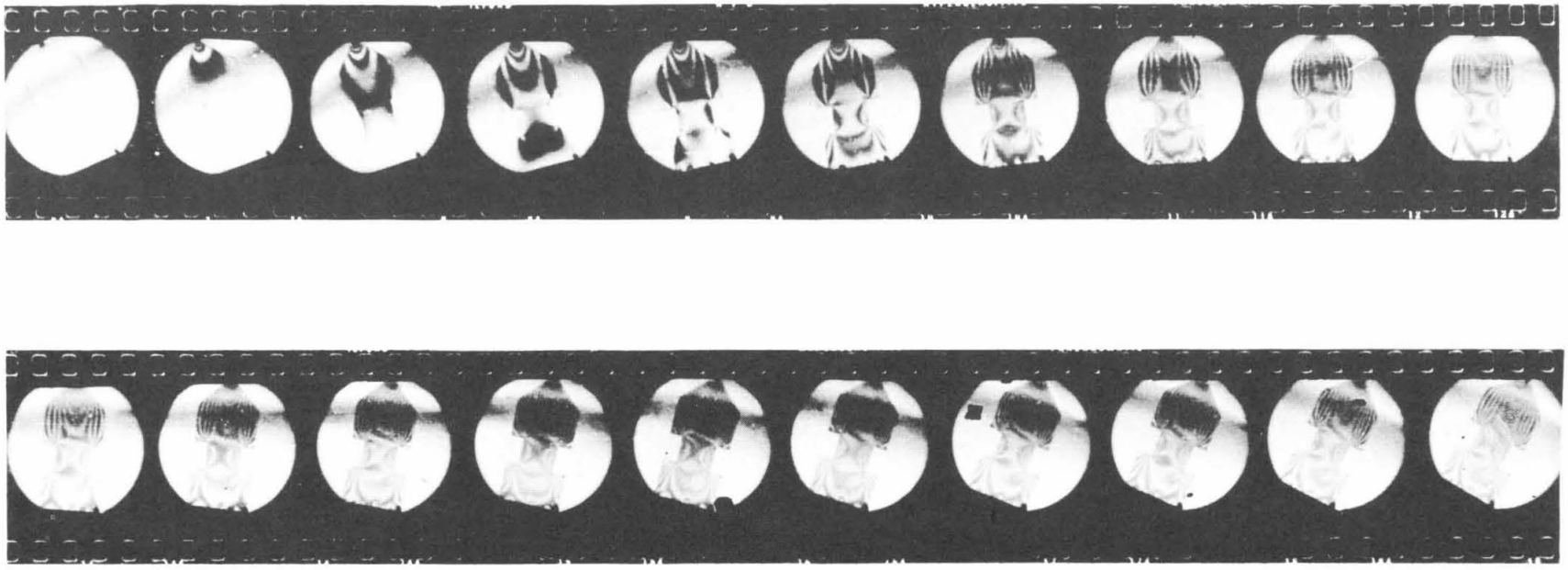


Figure 20. Dynamic Fringe Patterns for a 45° Notched Wedge-Body Configuration.

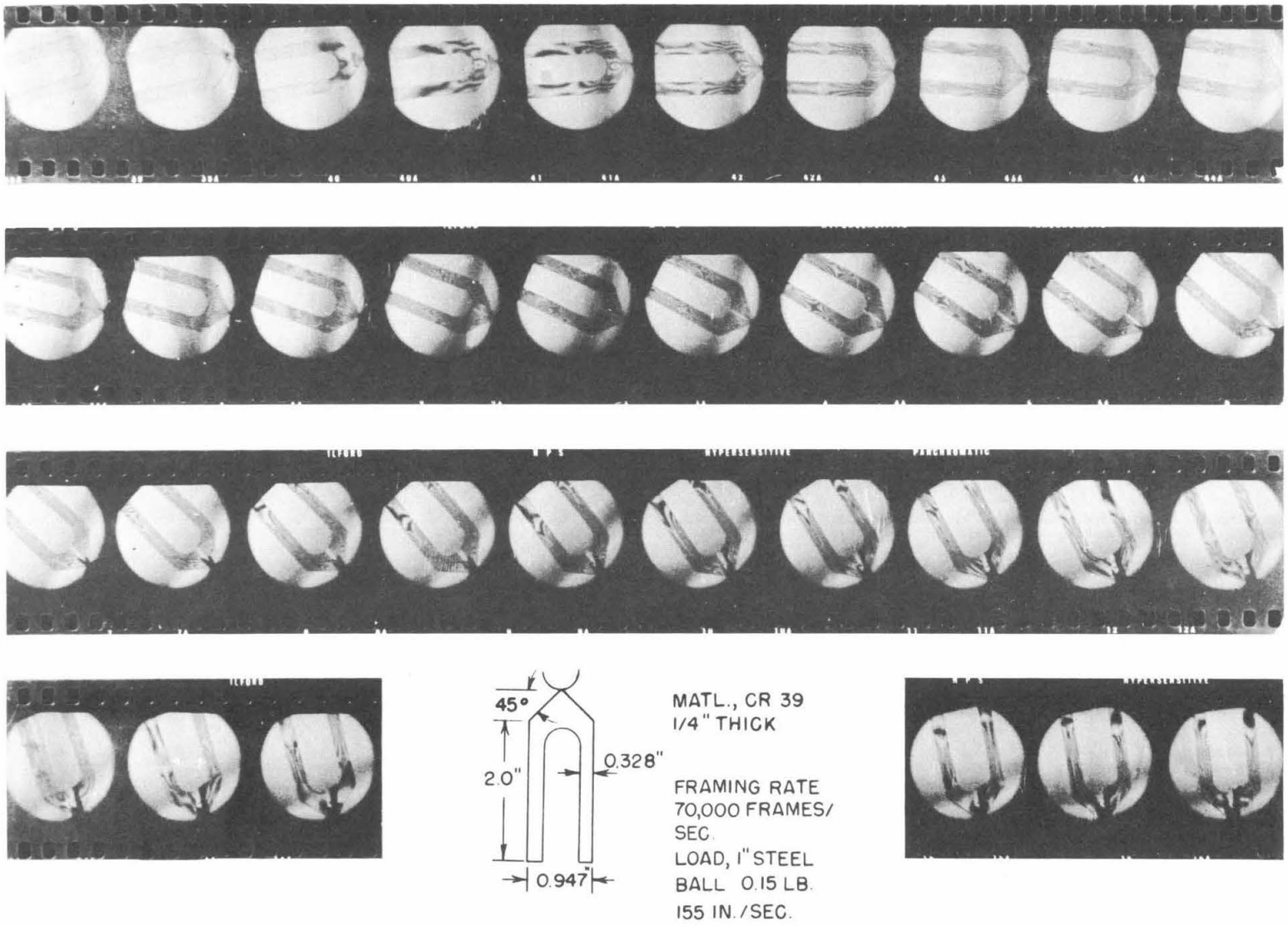


Figure 21. Dynamic Fringe Patterns in the Cross-Section of a Simulated Rocket Head.